

Capabilities and limitations of MISR aerosol products in dust-laden regions

Olga V. Kalashnikova^a, Michael J. Garay^b, Irina N. Sokolik^c, David J. Diner^a,
Ralph A. Kahn^c, John V. Martonchik^a, Jae N. Lee^a, Omar Torres^d,
Weidong Yang^d, Alexander Marshak^d, Sero Kassabian^a, and Mark Chodas^a

^a Jet Propulsion Laboratory, California Institute of Technology, Pasadena, CA, US

^b Raytheon Company, Pasadena, CA, US

^c Georgia Institute of Technology, Atlanta, GA

^d NASA Goddard Space Flight Center, MD

ABSTRACT

Atmospheric mineral dust particles have significant effects on climate and the environment, and despite notable advances in modeling and satellite and ground-based measurements, remain one of the major factors contributing to large uncertainty in aerosol radiative forcing. We examine the Multi-angle Imaging SpectroRadiometer (MISR) 11+ year aerosol data record to demonstrate MISR's unique strengths and assess potential biases of MISR products for dust study applications. In particular, we examine MISR's unique capabilities to 1) distinguish dust aerosol from spherical aerosol types, 2) provide aerosol optical depths over bright desert source regions, and 3) provide high-resolution retrievals of dust plume heights and associated winds. We show examples of regional and global MISR data products in dusty regions together with quantitative evaluations of product accuracies through comparisons with independent data sources, and demonstrate applications of MISR data to dust regional and climatological studies, such as dust property evolution during transport, dust source climatology in relation to climatic factors, and dust source dynamics. The potential use of MISR radiance data to study dust properties is also discussed.

Keywords: MISR, Terra, mineral dust, multiangle, remote sensing

1. INTRODUCTION

Dust outbreaks are a common feature of the world's arid and semi-arid regions. North African and East Asian dust storms have been documented for thousands of years, and these records have climate significance because dust storm frequency and severity affect soil moisture, air and surface temperatures, rainfall, and downwind air quality, and, at the same time, indicate the past/current climate change.^{1,2} There are many well-documented cases of dust from African sources being transported across the Atlantic and dust from East Asian sources in Mongolia and China being transported across the Pacific and even around the globe.^{3,4} During long-range transport dust particles can affect marine biochemistry by depositing iron in the ocean,^{5,6} play a role in neutralizing acid rain,⁷ affect the life cycle of coral reefs,⁸ and influence sea surface temperatures that impact hurricane formation and intensity.⁹ In order to advance the assessment of climate change projections due to dust effects and forcing, one of the foremost needs is to develop new techniques for interpreting and merging the diverse information from satellite remote sensing, in situ and ground-based measurements, and model simulations.¹⁰

MISR's multi-angular viewing geometry yields several geophysical products that can aid in understanding dust impacts on the climate system. The MISR instrument consists of nine cameras with view angles of $\pm 70.5^\circ$, $\pm 60.0^\circ$, $\pm 45.6^\circ$, $\pm 26.1^\circ$, and 0° (nadir), operating in four spectral bands centered at 446 nm (blue), 558 nm (green), 672 nm (red), and 867 nm (near infrared). The spatial resolution of the red band is 275 m in all nine cameras, the other bands are resampled to 1.1 km resolution in all the cameras, except the nadir, which

Further author information: (Send correspondence to Olga Kalashnikova)
Olga Kalashnikova: E-mail: Olga.Kalashnikova@jpl.nasa.gov, Telephone: 1 818-393-0469)

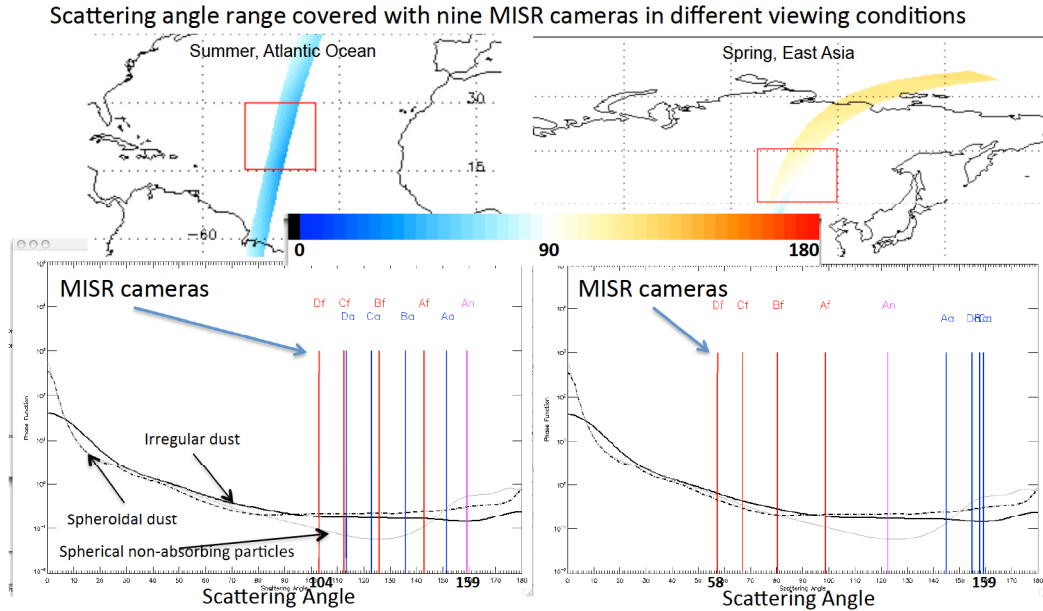


Figure 1. The MISR sampled scattering angle range depends on season and latitude. The upper plots shows the MISR scattering angle range during summer in the tropical Atlantic (104° to 159°) compared with Asia during spring (58° to 159°). The lower plots compare the observed MISR scattering angles (vertical lines) with example aerosol phase functions.

preserves the full 275 m resolution in all four bands. The common swath width is ~ 400 km and global coverage is obtained every nine days at the equator and more frequently at higher latitudes.¹¹

The MISR aerosol optical depth (AOD) product over bright land surfaces provides independent constraints on dust loadings in desert areas where other types of observations are sparse. In addition, the MISR aerosol product contains aerosol microphysical properties that could be used, to some extent, to distinguish dust from other aerosol types. MISR stereo data provide aerosol plume heights and associated wind vectors independent of any model constraints, and can be used to study dust dynamics. To illustrate MISR capabilities and evaluate product applicability to dust studies, we discuss MISR instrument sensitivity to dust properties, quantitatively evaluate aerosol product accuracies in dusty regions through comparisons with independent data sources, and assess MISR-derived dust climatologies.

2. DISTINGUISHING BETWEEN DUST AND OTHER AEROSOL TYPES

Multiangle, multispectral radiances observed by MISR enable distinguishing between spherical anthropogenic and non-spherical dust particles.¹²⁻¹⁴ Previous theoretical and case studies have demonstrated that under good viewing conditions over dark water the MISR aerosol retrieval is sensitive to differences in the angular-spectral signals of medium-mode dust shapes when the mid-visible AOD is larger than about 0.15, for components contributing 15-20% or more to the total AOD.¹⁵ The latest global assessment of MISR observations against collocated AERONET data also shows that the MISR Angstrom exponent could be used to distinguish aerosol types categorically for components representing about 20% of the total column AOD, provided the mid-visible AOD is larger than 0.15.¹⁶ The MISR aerosol retrieval algorithm can distinguish nonspherical dust from other spherical aerosol components as the instrument is sensitive to the angular distribution of the backscattered, top of atmosphere, radiances modified by the presence of dust particles.^{14,15} Therefore, the scattering angle range, scattering angle values, and the number of cameras available for aerosol retrievals should always be examined by users interested in the MISR AOD nonspherical fraction product. In the majority of dust-affected regions, the available number of cameras and the scattering angle range are sufficient to perform retrievals of AOD nonspherical fraction. As an example, Figure 1 shows the range of sampled scattering angles in Asia in spring and in the north Atlantic in summer. The lower plots indicate the scattering angle observed by each MISR

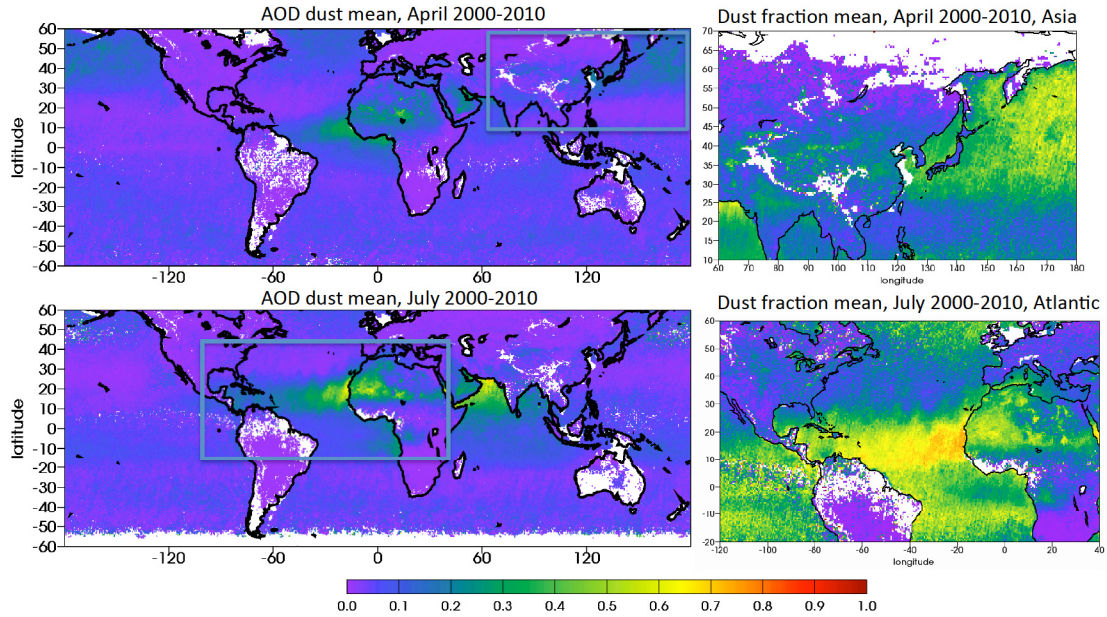


Figure 2. Mid-visible (558 nm) MISR dust AOD: 2000-2010 mean (left panels) and MISR dust fraction: 2000-2010 mean (right panels) for July (upper panels) and April (lower panels). MISR dust fraction is zoomed on the tropical Atlantic in July and the north Pacific in April.

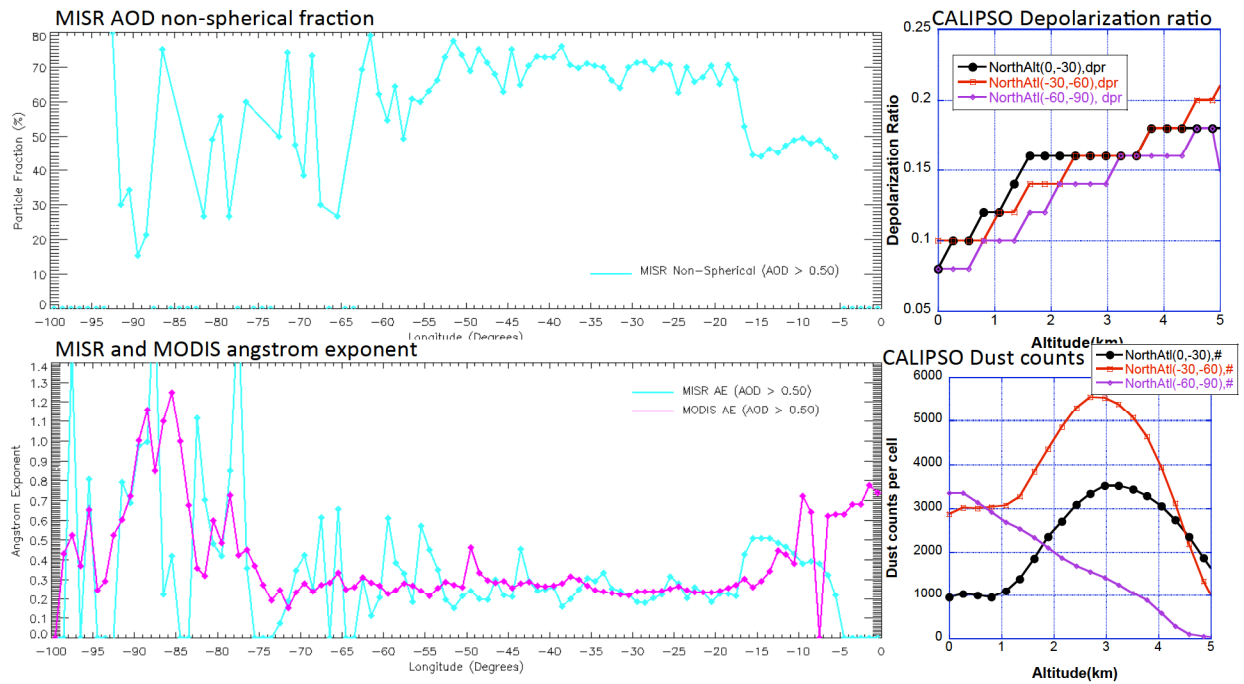


Figure 3. MISR July 2007 statistics of latitudinally averaged (0° to 40° latitude), (left panel): MISR AOD nonspherical fraction (upper left panel), and Angstrom exponent (lower left panel), both sub-setted for AOD 0.5. The lower left panel also plots the MODIS Angstrom exponent extracted from aerosol retrievals with a quality flag above 3; July 2007 statistics of CALIPSO depolarization ratio for all CALIPSO pixels identified as dust in the three selected boxes over the Atlantic: $[0-40N,0,-30W]$, $[0-40N,-30-60W]$, $[0-40N,-60-90W]$, (upper right panel); CALIPSO dust counts for all CALIPSO pixels identified as dust in the three selected boxes over the Atlantic: $[0-40N,0,-30W]$, $[0-40N,-30-60W]$, $[0-40N,-60-90W]$, (low right panel)

camera along with phase functions from three particles currently used in the MISR operational aerosol retrieval. Note the large difference between the spherical and non-spherical phase functions in the scattering angle range from 90° to 140° , which shows the distinguishability of these particle types.

The current operational MISR aerosol product (Version 22) reports the fraction of nonspherical particles retrieved over both land and water. However, the number of representative MISR and AERONET property retrievals coincident in time and space is limited, and is not statistically representative enough to perform a global validation of the nonspherical fraction. Therefore, we qualitatively examine the global MISR nonsphericity patterns obtained from 11+ years of observations to evaluate spatiotemporal distributions against known, climatological distributions of dust aerosol. As an example of our assessment, Figure 2 shows July and April global distribution of nonspherical AOD (nonspherical fraction weighted by AOD) gridded on a 0.5° grid and averaged over 11 years of observations (2000-2010). This is plotted together with MISR nonspherical fraction zoomed over the Atlantic Ocean in July and the Pacific in April. Figure 2 demonstrates that the MISR aerosol product identifies dust in the regions where dust is expected (e.g., over the Atlantic in July moving toward the Caribbean, over the Atlantic in April moving toward the Amazon, and over the Pacific in April moving toward the US west coast). However, some land-water discontinuity in the dust fraction is apparent. We can explain the observed discontinuity from results obtained from theoretical sensitivity studies. The MISR aerosol retrieval algorithm is sensitive to differences in the spectral signals of medium-mode dust with different composition (amount of hematite) at short visible wavelengths (blue and green), but there is very little difference in the spectral signature of dust of different compositions at wavelengths longer than $0.6 \mu\text{m}$. The current MISR aerosol retrieval algorithm uses two channels (red and near infrared) for water retrievals and 4 channels (blue, green, red, and near infrared) for land retrievals; therefore the retrieval sensitivity to dust composition changes across land-water boundaries. The dust model with a fixed refractive index that is currently used in the operational MISR aerosol look up table (LUT) is a valid assumption for 2-wavelength water retrievals; however, a wider range of dust models reflecting regional variability of dust chemistry (e.g., refractive index) likely needs to be included in the LUT to optimize the performance of 4-wavelength land retrievals in different parts of the globe. This behavior is also reflected in the current MISR nonspherical fraction, which appears to be more reliable over water than land, based on our climatological expectations. For example, the MISR nonspherical fraction in dust-dominant desert areas of East Asia only averages around 20%, which is unrealistically small (see Figure 2). It also should be noted that the MISR nonspherical fraction tends to be biased high at low AOD and therefore should typically be weighted by the corresponding total aerosol AOD.

MISR-derived aerosol nonsphericity is useful for studying the behavior of transported dust. However, note that relative changes in nonsphericity during dust transport are more reliable than the absolute dust nonspherical AOD values. We have demonstrated that MISR-constrained dust properties remain unchanged during five days of Transatlantic transport for the selected cases of dust sampled progressively downwind.¹⁷ Monthly statistics derived from currently available satellite aerosol products support this conclusion. For example, Figure 3 shows July 2000 statistics of latitudinally averaged MISR AOD nonspherical fraction and MISR Angstrom exponent both subsetted for AOD above 0.5. The MISR Angstrom exponent is plotted together with the latitudinally averaged MODIS Angstrom exponent. Figure 3 also shows the lidar depolarization ratio from CALIPSO for July 2007 for different parts of the Atlantic. Both the MISR nonspherical fraction and CALIPSO depolarization ratio remain similar across the Atlantic, eventually decreasing past 60° W longitude (after five days of dust transport), indicating the concentration of dust remains relatively constant during this period. MISR and MODIS also show an increase in the Angstrom exponent past 60° W. All these datasets indicate consistent behavior of the transported dust as it moves from the west coast of Africa, into the Saharan Air Layer (SAL) where it remains trapped, and finally into the eastern Atlantic where the SAL erodes and the dust is mixed downward to the surface. Therefore MISR nonspherical fraction for AOD above 0.5 correctly captures relative changes in the dust fraction during transport across Atlantic. The MISR nonspherical fraction is not expected to perform as well over the much cloudier Pacific Ocean due to reduced sampling and the widespread sub-visible cirrus ice clouds those nonspherical particle shapes might complicate MISR aerosol retrievals.

3. AOD CLIMATOLOGY OVER BRIGHT SURFACES

The performance of the operational MISR aerosol retrieval over bright desert sources and its sensitivity to near-surface aerosols and surface properties have been validated and used over many desert surfaces.¹⁸⁻²⁵ A global

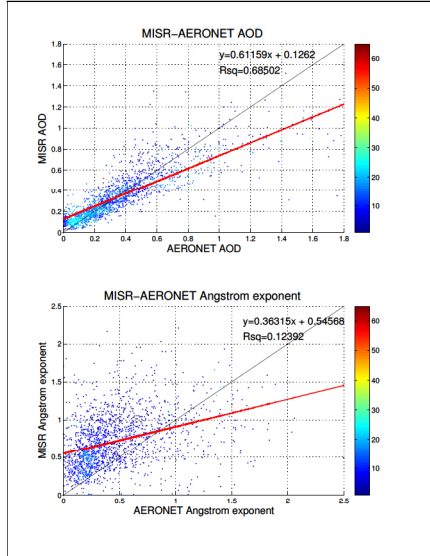


Figure 4. Mid-visible (558 nm) MISR vs. AERONET coincident AOD and Angstrom exponent density scatter-plots: West Africa, 2000-2010

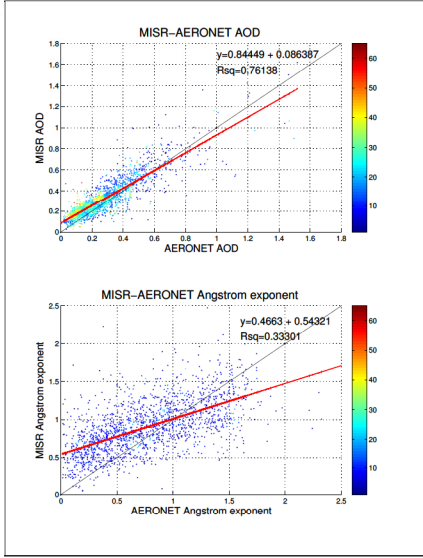


Figure 5. Mid-visible (558 nm) MISR vs. AERONET coincident AOD and Angstrom exponent density scatter-plots: East Africa and Middle East, 2000-2010

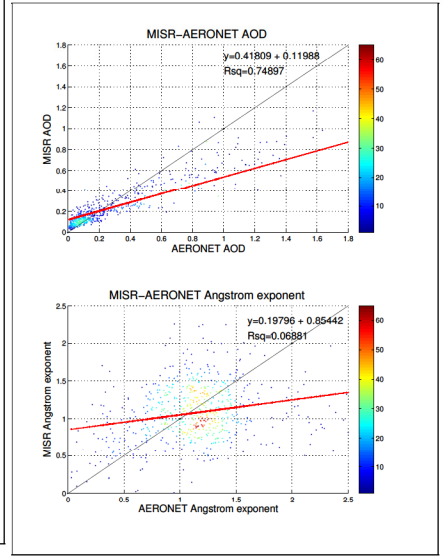


Figure 6. Mid-visible (558 nm) MISR vs. AERONET coincident AOD and Angstrom exponent density scatter-plots: East Asia, 2000-2010

Table 1. AERONET sites used in the regression analysis presented in Figures 3, 4, and 5

West Africa	East Asia	East Africa and Middle East
Agoufou, Banizoumbou	Beijing	Abu Al Bukhoosh, Abu Dhabi
Capo Verde, DMN Maine Soroa	Dalanzadgad	Al Dhafra, Al Ain
Dahkla, Dakar	Inner Mongolia	Al Khaznah, Al Qlaa
IER Cinzana, Izana	PKU PEK	Bahrain, Cairo EMA
La Laguna, Niamey	XiangHe	Cairo University, Dalma
Ouagadougou	Xinglong	Dhabi, Dhadnah
Praia	Yufa PEK	Eilat, Hamim
Quarzazate		Jabal Hafeet, Mezaira
Ras El Ain		Muscat, Mussafa
Saada		Nes Ziona, SEDE BOKER
Santa Cruz Tenerife		SMART, SMART POL
Tamanrasset INM		Saih Salam, Sir Bu Nuair
Zinder DMN		Solar Village, Umm Al Quwain

comparison of coincident MISR and AERONET sunphotometer data showed that overall, about 70% to 75% of MISR AOD retrievals fall within 0.05 or 20% \times AOD, and about 50% to 55% are within 0.03 or 10% \times AOD, except at sites where dust or mixed dust and smoke are commonly found.^{16,26} Figures 4, 5, and 6 show density plots and regression statistics of all available 2000-2010 MISR mid-visible AOD and MISR Angstrom exponent against coincident AERONET measurements in the 3 \times 3 nearest 17.6 km MISR aerosol retrieval regions and within 1 hour of the MISR overpass in West Africa, the arid areas in Middle East, and East Asia, respectively. The AERONET stations used in the regressions for each region are listed in Table 1. Consistent with previous, global studies, MISR retrievals in all three selected dust-dominated regions tend to overestimate

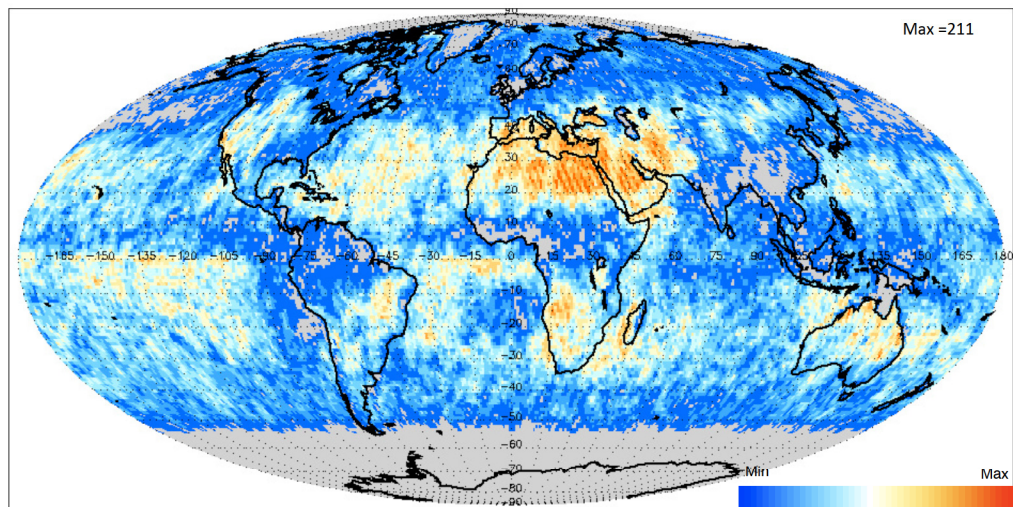


Figure 7. MISR valid retrieval count in a $1^\circ \times 1^\circ$ global grid, July 2007

instantaneous AOD in the low AOD range and underestimate it in the high range compared to AERONET. The AOD underestimation slope depends on the region, and varies from underestimation at AODs above 1.5 in the Middle East to an underestimation at AODs above 0.5 in East Asia. A greater diversity of dust optical models is needed to better represent different desert source regions, though other factors might also be involved. MISR is sensitive to 3-5 groupings of particle size under good retrieval conditions; as such, the Angstrom exponent density plots show that both MISR and AERONET Angstrom exponents are dominated by large particles, with values predominantly below 0.5 in West Africa, where coarse dust is most common, and indicating medium particles with values around one in East Asia, where dust is often mixed with a local pollution and biomass burning aerosol particles.

Recent studies have shown that the operational MISR aerosol product provides reliable climatologies in Africa and the Middle East.^{27,28} Determining dust climatological patterns in East Asia with the MISR aerosol product, however, is difficult, because frequent cloud cover in this region reduces the number of valid retrievals. Figure 7 shows an example of the number of valid aerosol retrievals available in a $1^\circ \times 1^\circ$ global grid for July 2007. MISR sampling studies have shown that for East Asia, averaging over at least a $10^\circ \times 10^\circ$ area is required to obtain daily AOD time series with no sampling gaps. However, MISR interannual and seasonal AOD patterns reproduce those at AERONET stations across Asia, and agree with independent satellite data in dust source regions. MISR monthly anomalies in Asian dust source regions are in agreement with those derived from MODIS Deep Blue and OMI AOD, if weighted by the measurement standard deviation, and, in turn, show correlation with the Niño 3.4 index as demonstrated in Figure 8. MISR mean AOD spatial patterns indicate higher dust loadings in the Taklamakan Desert during La Niña years vs. El Niño years. These observations support reported model predictions of the effect of El Niño on transported Asian dust.²⁹

4. DUST PLUME DYNAMICS

MISR aerosol plume top height and wind information are derived at a spatial resolution of 1.1×1.1 km by analysis of the MISR radiance data using the MISR INteractive eXplorer (MINX) tool.^{30,31} MINX provides an interface within which a trained user can outline dust plumes and provide a wind direction. Inclusion of the wind direction reduces the number of free parameters in the simultaneous stereoscopic retrieval of heights and winds from MISR data, allowing precise retrievals of the plume height and wind speed. Uncertainties in the plume heights are estimated to be ~ 200 m, and uncertainties in the wind speed are $\sim 1-2 \text{ ms}^{-1}$.³¹ As these high-resolution, spatially extensive measurements of dust plume-top heights are obtained geometrically, they are unaffected by background aerosols and thin cirrus, atmospheric thermal structure (e.g. temperature inversions), cloud emissivity, or instrument radiometric calibration. Figure 9 shows two examples of comparison MINX dust

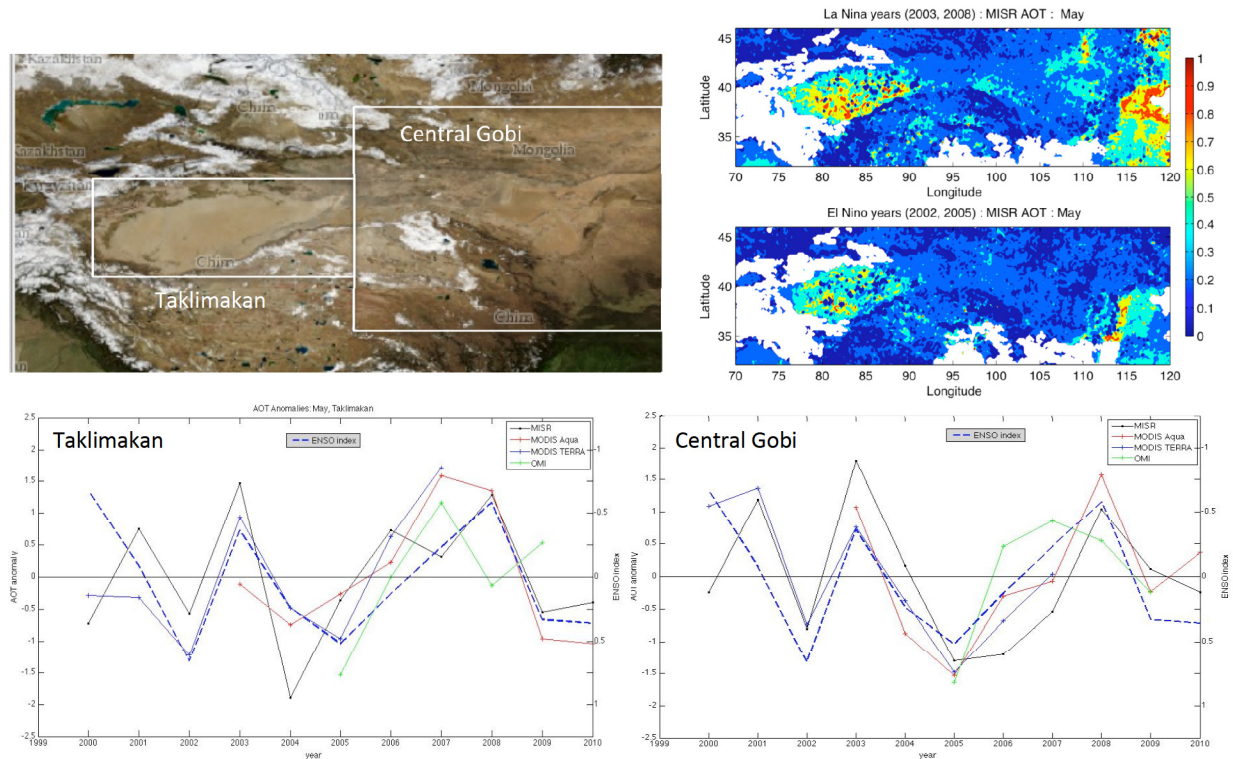


Figure 8. East Asian dust source map (upper left panel); MISR mean AOD in May averaged over La Niña (2003,2008) and El Niño (2002,2005) years (upper right panel); Normalized May AOD anomalies derived from Level 2 monthly MISR, MODIS-Terra Deep Blue (quality flag above 3), MODIS-Aqua Deep Blue (quality flag above 3), and OMI AOD product in the Taklamakan (lower left panel) and Central Gobi (lower right panel) plotted together with May Niño 3.4 index.

plume height with a nearly-coincident (3 hours difference) CALIPSO observations of the same dust events: one in the Bodélé dust source region and one over the Atlantic off the Saharan coast. In the first case, both MISR and CALIPSO place the dust layer at ~ 1 km altitude. In the second case, they both find the dust layer around 5 km. Note that the agreement is within the estimated 200 m uncertainty in the MINX retrieval (the CALIPSO vertical resolution is 30 m). This figure shows that the MINX measurement uncertainty is applicable for dust plumes as well as for smoke plumes, which have been investigated previously.

To demonstrate the application of MISR stereo data to the study of dust plume dynamics, we employ the MINX software tool to calculate dust plume heights and associated wind speeds in the Bodélé source region for all events observed by MISR from March 2000 through March 2010 (over 500 events). A remarkable combination of geography and climate makes the Bodélé depression the world's largest dust source. Downward mixing of persistent nocturnal low level jet winds in the early to mid-morning generates strong dust outbreaks observed by many satellite instruments.^{32,33} MISR passes over the Bodélé around 10:30 a.m. local time, near the time of peak activity. Figure 10 shows the MISR plume height and wind speed climatology in the Bodélé depression. Seasonally, MISR data indicate an increase in plume heights during the summer months, most likely due to the deepening of the boundary layer caused by increasing surface temperature. MISR also observes an increase of wind speeds in the winter and spring seasons, in agreement with the reported increase in dust events during the winter.^{32,33} Mean plume heights were found to vary with season from 400 m to 900 m above the ground level and the mean wind speed is found to be 14 ms^{-1} . The MISR dust plume height and wind statistics may provide valuable constraints for testing and refining regional dust modeling systems and dust emission and lifting parameterizations within GCMs.

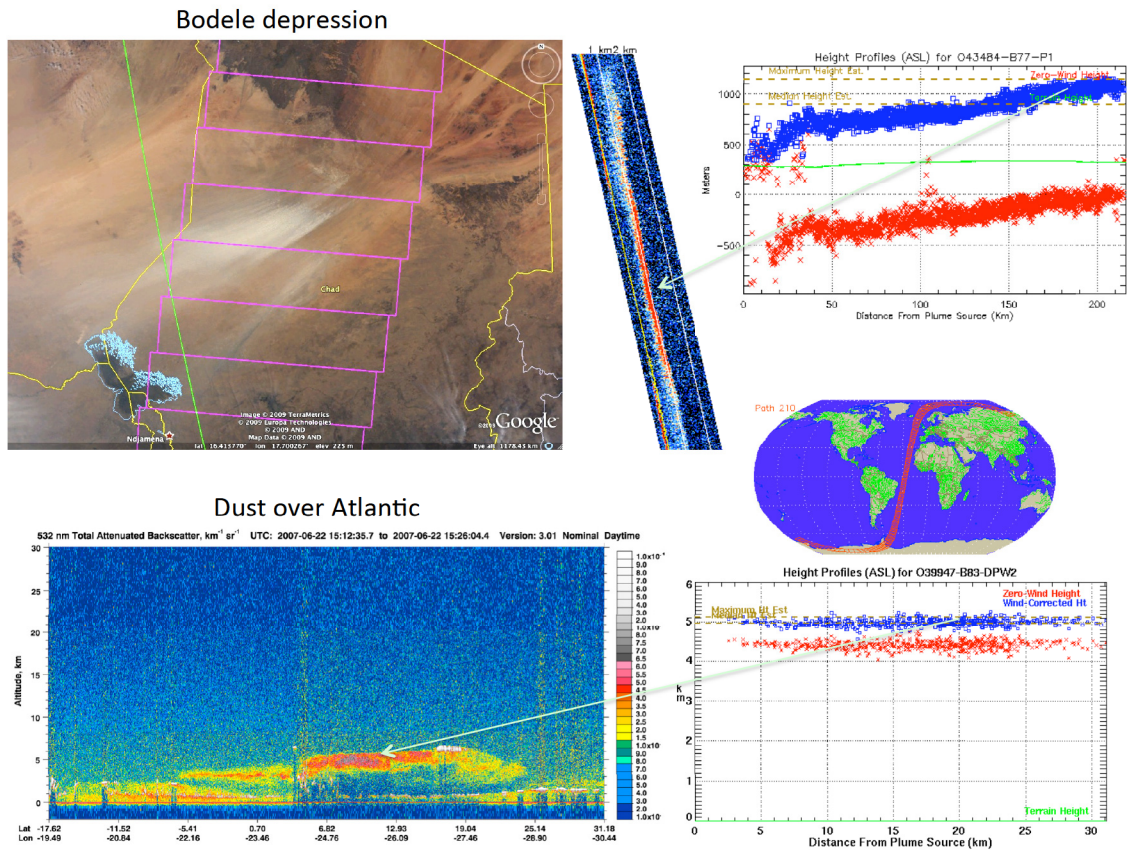


Figure 9. The comparison MISR MINX dust plume heights with a nearly-coincident (3 hours difference) CALIPSO measurements of aerosol extinction: Dust event over the Bodélé depression on February 20, 2008 (upper panel) and a dust event off the Saharan coast on June 22, 2007.

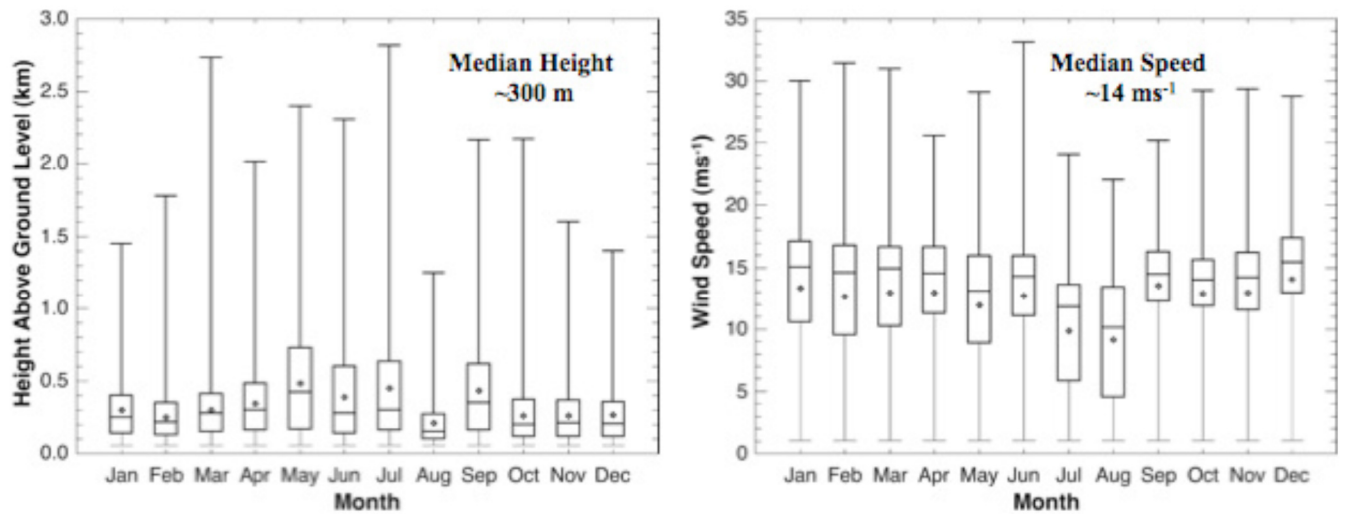


Figure 10. MISR plume height (left panel) and wind speed (right panel) monthly climatology in the Bodélé depression obtained from 512 cases of MISR stereophotogrammetric MINX retrievals.

5. CONCLUSIONS AND OUTLOOK

Analysis of the current (Version 22) MISR aerosol products shows that: 1. the MISR nonspherical fraction product performs well over the water in terms of relative changes of dust fraction during transport over the Atlantic ocean, 2. MISR AOD retrievals fall within 0.05 or $20\% \times \text{AOD}$ in the low AOD range (AOD less than 0.5) in the arid dust-laden regions of North Africa, Middle East, and East Asia, 3. MISR derived dust plume heights and wind climatologies provide valuable insights on dust source dynamics. However, some algorithm upgrades are needed to correct systematic AOD and AOD nonspherical fraction underestimation for high AOD situations over bright land, and land-water discontinuity in AOD nonspherical fraction globally. Sensitivity studies also indicate that multispectral radiances in MISR's blue and green wavelengths, currently not used in MISR water retrievals, could potentially provide valuable information for the study of dust properties such as dust hematite content and dust size distributions.

ACKNOWLEDGMENTS

We thank the MISR team for offering facilities, access to data, and useful discussions. The work of O. V. Kalashnikova is supported by in part by the NASA Earth Sciences Division, Climate and Radiation program, and in part by the NASA Earth Observing System Multiangle Imaging SpectroRadiometer project, D. J. Diner, Principal Investigator. This work was performed at the Jet Propulsion Laboratory, California Institute of Technology, under contract with NASA. The MISR data were obtained from the NASA Langley Research Center Atmospheric Sciences Data Center.

REFERENCES

- [1] Sun, J., Zhang, M., and Liu, T., "Spatial and temporal characteristics of dust storms in china and its surrounding regions, 1960–1999: Relations to source area and climate," *J. Geophys. Res.* **106**, 10325–10333 (2001).
- [2] Shao, Y. and Dong, C. H., "A review on east asian dust storm climate, modelling and monitoring," *Global and Planetary Change* **52**, 1–22 (2006).
- [3] Eguchi, K., Uno, I., Yumimoto, K., Takemura, T., Shimizu, A., Sugimoto, N., and Liu, Z., "Trans-pacific dust transport: integrated analysis of NASA/CALIPSO and a global aerosol transport model," *Atmos. Chem. Phys.* **9**, 3137–3145 (2009).
- [4] Uno, I., Eguchi, K., Yumimoto, K., Takemura, T., Shimizu, A., Uematsu, M., Liu, Z., Wang, Z., Hara, Y., and Sugimoto, N., "Asian dust transported one full circuit around the globe," *Nature Geosci.* **2**, 557–560 (2009).
- [5] Martin, J. H., Fitzwater, S. E., and Gordon, R. M., "We still say iron deficiency limits phytoplankton growth in the subarctic pacific," *J. Geophys. Res.*, **96**(C11), 206992,700 (1991).
- [6] Bopp, L., Kohfeld, K. E., Qur, C. L., and Aumont, O., "Dust impact on marine biota and atmospheric co₂ during glacial periods," , *Paleoceanography* **18**, 10.1029/2002PA000810 (2003).
- [7] Wang, Z., Akimoto, H., and Uno, I., "Neutralization of soil aerosol and its impact on the distribution of acid rain over east asia: Observations and model results," *J. Geophys. Res.* **107**(D19)(4389), doi:10.1029/2001JD001040 (2002).
- [8] Shinn, E. A., Smith, G. W., Prospero, J. M., Betzer, P., Hayes, M. L., Garrison, V., and Barber, R. T., "African dust and the demise of caribbean coral reefs," *Geophys. Res. Lett.*, **27**,(19), 30293032 (2000).
- [9] Dunion, J. P. and Velden, C. S., "The impact of the saharan air layer on atlantic tropical cyclone activity," *Bulletin of the American Meteorological Society* **85**, doi:10.1175/BAMS853353 (2004).
- [10] Sokolik, I. N., Winker, D. M., Bergametti, G., Gillette, D. A., Carmichael, G., Kaufman, Y. J., Gomes, L., Schuetz, L., , and Penner, J. E., "Introduction to special section: Outstanding problems in quantifying the radiative impacts of mineral dust," *J. Geophys. Res.* **106**(D16), 18,01518,028 (2001).
- [11] Diner, D. J., Beckert, J. C., Bothwell, G., and Rodriguez, J., "Performance of the misr instrument during its first 20 months in earth orbit," *IEEE Trans. Geosci. Rem. Sens.* **40**, 1449 (2002).
- [12] Kahn, R. A., West, R., McDonald, D., Rheingans, B., and Mishchenko, M., "Sensitivity of multi-angle remote sensing observations to aerosol sphericity," *J. Geophys. Res.* **102**, 16,86116,870 (1998).

- [13] Kahn, R., Banerjee, P., and McDonald, D., "The sensitivity of multiangle imaging to natural mixtures of aerosols over ocean," *J. Geophys. Res.* **106**, 18,21918,238. (2001).
- [14] Kalashnikova, O. V., Kahn, R. A., Sokolik, I. N., and Li, W.-H., "The ability of multi-angle remote sensing observations to identify and distinguish mineral dust types: Part 1. optical models and retrievals of optically thick plumes," *J. Geophys. Res.* **Vol. 110**, doi:10.1029/2004JD004550 (2005).
- [15] Kalashnikova, O. V. and Kahn, R. A., "Ability of multiangle remote sensing observations to identify and distinguish mineral dust types: Sensitivity over dark water," *J. Geophys. Res.* **111**(D11207), doi:10.1029/2005JD006756 (2006).
- [16] Kahn, R. A., Gaitley, B., Garay, M., Diner, D., Eck, T., Smirnov, A., and Holben, B., "Misr aerosol product assessment by comparison with aeronet," *J. Geophys. Res.* **115**(D23209), doi:10.1029/2010JD014601 (2010).
- [17] Kalashnikova, O. V. and Kahn, R. A., "Mineral dust plume evolution over the atlantic from combined misr/modis aerosol retrievals," *J. Geophys. Res.* **113**(D24204), doi:10.1029/2008JD010083 (2008).
- [18] Martonchik, J. V., Diner, D. J., Kahn, R., Gaitley, B., and Holben, B., "Comparison misr and aeronet aerosol optical depth over desert sites," *Geophys. Res. Lett.* **31**, doi:10.1029/2004GL019807 (2004).
- [19] Christopher, S. A., Gupta, P., and Haywood, J., "Aerosol optical thicknesses over north africa: 1. development of a product for model validation using ozone monitoring instrument, multiangle imaging spectroradiometer, and aerosol robotic network," *J. Geophys. Res.* **113**(D00C04), doi: 10.1029/2007JD009446 (2008).
- [20] Christopher, S. A., Johnson, B., Jones, T., and Haywood, J., "Vertical and spatial distribution of dust from aircraft and satellite measurements during the gerbils field campaign," *Geophys. Res. Lett.* **36**(L06806), doi:10.1029/2008GL037033 (2009).
- [21] Frank, T. D., Girolamo, L. D., and Geegan, S., "The spatial and temporal variability of aerosol optical depths in the mojave desert of southern california," *Rem. Sens. Environ* **107**, 54–64 (2007).
- [22] Kahn, R., Petzold, A., Wendisch, M., Bierwirth, E., Dinter, T., Esselborn, M., Fiebig, M., Heese, B., Knippertz, P., Muller, D., Schladitz, A., and von Hoyningen-Huene, W., "Desert dust aerosol air mass mapping in the western sahara, using particle properties derived from space-based multi-angle imaging," *Tellus* **61**, 239–251 (2009).
- [23] Koven, C. D. and Fung, I., "Identifying global dust source areas using high-resolution land surface form," *J. Geophys. Res.* **113**(D22204), doi:10.1029/2008JD010195 (2008).
- [24] Xia, X. G., Wang, P. C., and Wang, Y. S., "Aerosol optical depth over the tibetan plateau and its relation to aerosols over the taklimakan desert," *Geoph. Res. Lett.* **35**(16), L16804 (2008).
- [25] Xia, X. G. and Zong, X., "Shortwave versus longwave direct radiative forcing by taklimakan dust aerosols," *Geophys. Res. Lett.* **36**(L07803) (2009).
- [26] Kahn, R., Gaitley, B., Martonchik, J., Diner, D., Crean, K., and Holben, B., "Misr global aerosol optical depth validation based on two years of coincident aeronet observations," *J. Geophys. Res.* **110**(, D104), doi:10.1029/2004JD004706 (2005).
- [27] Marey, H. S., J. C. Gille, H. M. E.-A., Shalaby, E. A., and El-Raey, M. E., "Aerosol climatology over nile delta based on modis, misr and omi satellite data," *Atmos. Chem. Phys. Discuss.* **11**, 1044910484 (2011).
- [28] Yigiletu, M. T., Sivakumar, V., Botai, J. O., and Mengistu, G., "Aerosol climatology over south africa based on 10 years of multi-angle imaging spectroradiometer (misr) data," *J. Geophys. Res.* , doi:10.1029/2011JD016023 (2011).
- [29] Gong, S. L., Zhang, X. Y., Zhao, T. L., Zhang, X. B., Barrie, L. A., McKendry, I. G., and Zhao, C. S., "A simulated climatology of asian dust aerosol and its trans-pacific transport. part ii: Interannual variability and climate connections," *Journal of Climate* **19**(1), 104–122 (2006).
- [30] Nelson, D., Averill, C., Boland, S., Morford, R., Garay, M., Rheingans, B., Thompson, C., Hall, J., Diner, D., and Campbell, H., "Misr interactive explorer (minx) v1.0 users guide," *JPL reports D-41552*(available from: <http://www.openchannelsoftware.com/projects/MINX>) (2008).
- [31] Nelson, D. L., Chen, Y., Kahn, R. A., Diner, D. J., and Mazzoni, D., "Example applications of the misr interactive explorer (minx) software tool to wildfire smoke plume analyses," *Proc. SPIE* **7089**, doi:10.1117/12.795087 (2008).

- [32] Washington, R., Todd, M. C., Engelstaedter, S., Mbainayel, S., and Mitchell, F., “Dust and the low-level circulation over the Bodélé Depression, Chad: Observations from BoDEX 2005,” *J. Geophys. Res.* **111**, D03201, doi:10.1029/2005JD006502 (2006).
- [33] Todd, M. C., Washington, R., Martins, J. V., Dubovik, O., Lizcano, G., M’Bainayel, S., and Engelstaedter, S., “Mineral dust emission from the Bodélé Depression northern Chad, during BoDEX 2005,” *J. Geophys. Res.* **112**, D06207, doi:10.1029/2006JD007170 (2007).